ISSN 1063-7729, Astronomy Reports, 2022, Vol. 66, No. 6, pp. 500–512. © Pleiades Publishing, Ltd., 2022.
Russian Text © The Author(s), 2022, published in Astronomicheskii Zhurnal, 2022, Vol. 99, No. 6, pp. 506–519.

Accounting for the Yarkovsky Effect in Reference Frames Associated with the Radius Vector and Velocity Vector

T. N. Sannikova*

Crimean Astrophysical Observatory, Russian Academy of Sciences, Nauchnyi, Crimea, Russia

**e-mail: tnsannikova@craocrimea.ru*

Received March 11, 2022; revised March 31, 2022; accepted March 31, 2022

Abstract—The motion of an asteroid in a central gravitational field in the presence of an additional perturbing acceleration due to the Yarkovsky effect was considered. The long-term evolution of the orbit was studied using the analytical solution of the averaged equations of motion in two orbital frames of reference: $\mathbb{O}_1$, associated with the radius vector, and $\mathbb{O}_2$, associated with the velocity vector. The Yarkovsky acceleration components were found as averages over the orbital period based on the thermophysical characteristics and rotation parameters of a small body within the linear thermophysical model of the Yarkovsky force for spherical asteroids. The drifts of the mean anomaly and semimajor axis, as well as the displacement relative to the unperturbed position per 1000 orbital revolutions, were obtained for model asteroids with different orbital eccentricities in both frames of reference. As a result, the drifts of the semimajor axis and the mean anomaly, as well as the displacements, were found to differ by less than 1% at small eccentricities (up to 0.5). When $e_0 > 0.5$, the values found in system $\mathbb{O}_1$ are always greater than the same values in system $\mathbb{O}_2$. At $e_0 \sim 0.5$–0.7, their difference does not exceed 6%, gradually increasing with the growth of e_0. For $e_0 > 0.7$, these differences increase exponentially. Thus, when the Yarkovsky effect is modeled with transversal acceleration, the expected values of drifts and displacements for objects with highly elliptical orbits may be overestimated, which may be one of the factors for the low detection of the Yarkovsky effect directly from astrometric observations.

Keywords: general questions of celestial mechanics, Yarkovsky effect, tangential acceleration, transversal acceleration, radial acceleration, normal acceleration, drift of the semimajor axis, drift of the mean anomaly, displacement relative to the unperturbed position, near-Earth asteroids

DOI: 10.1134/S1063772922070058

1. INTRODUCTION

At present, humanity has come to recognize the reality of the threat of a collision between the Earth and small bodies of the Solar System. To prevent this threat, it is necessary to identify potentially dangerous objects, determine their orbits, and assess the probability of their collision or close encounter with the Earth. To improve the accuracy of predicting the motion of a body, it is necessary to consider non-gravitational effects, in particular, the Yarkovsky effect. This effect occurs due to the thermal radiation of a rotating body with non-zero thermal inertia, and it causes secular variations in the eccentricity, semimajor axis and, first of all, the mean anomaly, the variation of which increases quadratically with time. Thus, the Yarkovsky effect plays a significant role in the evolution of the orbits of small bodies; therefore, determining the magnitude of this effect and studying its impact on near-Earth asteroids (NEAs) is necessary for calculating their orbits and assessing their potential hazard to the Earth. Also, the Yarkovsky effect is considered one of the reasons for the migration of asteroids to the resonance zones of the Main Belt, after which they may replenish the NEA population. In addition, covering the object with a special substance to change its orbit using the Yarkovsky effect is proposed as one of the ways to manipulate space objects that threaten to collide with the Earth.

To take into account the Yarkovsky effect and study its influence on the long-term evolution of the orbit of a small body, it is necessary to know the values of the components of the perturbing acceleration that occurs due to this effect. At present, the most common method for estimating the Yarkovsky effect is differential orbit correction [1–4]. Since the Yarkovsky effect leads to secular perturbations of the semimajor axis, transversal acceleration is used in the following form

$$\mathbf{a}_t = A_2 \left(\frac{r_0}{r}\right)^2 \hat{\mathbf{t}},$$

where r is the heliocentric distance to the asteroid, $r_0 = 1$ AU, and A_2 is the dynamic parameter deter-

mined in the orbital fitting with the orbital elements. Furthermore, the drift of the semimajor axis of the orbit is estimated, and this drift is considered when predicting the motion of the asteroid. However, when the effect is determined by this method, a significant part of it remains unaccounted, which can cause noticeable errors in predicting the motion of a body based on the resulting orbit [5].

A more accurate method, in our opinion, is the calculation of the acceleration components based on some model of the Yarkovsky force. At present, extensive work is underway to determine the thermophysical characteristics of small bodies using observations obtained in ground-based and orbital observatories, for example, determining the shape and rotation parameters of asteroids from their photometry [6, 7], determining the diameter and geometric albedo from the total thermal radiation of bodies found as a result of a four-band thermal infrared all-sky survey carried out by an infrared telescope located in near-Earth orbit (NEOWISE project) [8], or refining the thermal characteristics of the surface during laboratory studies of meteorite and asteroid samples [9], as well as during space missions to asteroids [10–12]. In the future, as the knowledge about the properties of small bodies expands, explicit consideration of the Yarkovsky effect will become more preferable.

As mentioned above, when estimating the drift of the semimajor axis due to the Yarkovsky effect, the perturbing acceleration is usually modeled with a transversal component. However, the tangential acceleration component has a more direct effect on the variation in the object's velocity and, as a result, on the drifts of the semimajor axis and the mean anomaly. This is not essential for circular orbits and small eccentricities, when the transversal and tangential components almost coincide. However, for highly elliptical orbits, the situation is different. It is also obvious that the magnitude of the variation in the orbital elements should not depend on the choice of the reference frame. Furthermore, we determine the element drifts and the displacement relative to the unperturbed position per 1000 orbital revolutions for model asteroids with thermophysical characteristics similar to the asteroid 101955 Bennu, but with different orbital eccentricities in two orbital systems and compare them.

For this purpose, let us consider the motion of a zero-mass point $\mathcal{A}$ (asteroid) under the influence of attraction to the central body $\mathcal{S}$ (Sun) and perturbing acceleration $\mathbf{P}'$, which is inversely proportional to the distance to $\mathcal{S}$ squared, i.e., $\mathbf{P}' = \mathbf{P}/r^2$, and its value is small compared to the main acceleration $\varkappa^2/r^2$:

$$\max\frac{|\mathbf{P}'|}{\varkappa^2 r^{-2}} = \max\frac{|\mathbf{P}|}{\varkappa^2} = \mu \ll 1. \qquad (1)$$

Here, $\mathbf{r} = \mathcal{S}\mathcal{A}$, $r = |\mathbf{r}|$, $\varkappa^2$ is the product of the gravitational constant and mass $\mathcal{S}$, and μ is a small parameter. Let the acceleration $\mathbf{P}'$ be due to the Yarkovsky effect. In this case, condition (1) is satisfied, since for an NEA with a diameter below 1 km, the typical value of the transversal parameter $A_2 \sim 10^{-15}$–10^{-13} AU/day^2, and for a distance of 1 AU, $\mu \approx 10^{-9} \ll 1$. The vector $\mathbf{P}$ components are constant and small (on the order of μ) values. For this problem, the authors of [13] obtained evolutionary equations of motion in the mean elements in the first order of smallness in μ for various frames of reference. In [14, 15], these equations are integrated for two orbital frames of reference: $\mathbb{O}_1$, associated with the radius vector, and $\mathbb{O}_2$, associated with the velocity vector. Section 2 presents particular solutions needed to study the long-term evolution of the semimajor axis and the mean anomaly.

Let us consider two reference systems with the origin at $\mathcal{S}$: $\mathbb{O}_1$ with the axes oriented along the radius vector, transversal (perpendicular to the radius vector in the plane of the osculating orbit along the direction of motion), and binormal (along the area vector), and $\mathbb{O}_2$ with the axes along the velocity vector, normal to it in the plane of the osculating orbit, and the binormal. Let vector $\mathbf{P}$ have components P_r, P_t, P_n in system $\mathbb{O}_1$ and $P_{\mathfrak{T}}$, $P_{\mathfrak{N}}$, P_n in $\mathbb{O}_2$. We denote the values of the vector $\mathbf{P}$ components averaged over the orbital period as follows: $S = \overline{P}_r$, $T = \overline{P}_t$, $\mathfrak{T} = \overline{P}_{\mathfrak{T}}$, $\mathfrak{N} = \overline{P}_{\mathfrak{N}}$, $W = \overline{P}_n$ and call them the radial, transversal, tangential, normal, and binormal parameters, respectively. In [16], the corresponding expressions are derived for the parameters S, T, W based on the formulas for the components of the Yarkovsky acceleration in the projection onto the system $\mathbb{O}_1$ axes obtained in the linear thermophysical model of the Yarkovsky force for spherical asteroids [17] and published in [18]. In this paper, the tangential $\mathfrak{T}$ and normal $\mathfrak{N}$ parameters are derived (see Section 3).

In Section 4, the drifts of the semimajor axis and the mean anomaly, as well as the displacement relative to the unperturbed position due to the Yarkovsky effect, are found and compared for model asteroids in two orbital reference systems.

2. EQUATIONS OF MOTION

As shown in [16], the binormal component P_n averaged over the orbital period is zero ($W = 0$), so we use particular analytical solutions.

For reference frame $\mathbb{O}_1$ [14]:

$$t = \frac{\varkappa^2}{n_0 T}\left(\frac{\eta_0}{1-\eta_0}\right)^3\left(2\ln\frac{\eta}{\eta_0} + \frac{1}{\eta} - \eta - \frac{1}{\eta_0} + \eta_0\right),$$

$$a = a_0\left[\frac{\eta_0(1-\eta)}{\eta(1-\eta_0)}\right]^2,$$
$$i = i_0, \quad \Omega = \Omega_0, \quad \omega = \omega_0, \tag{2}$$
$$M = M_0 + \frac{\varkappa^2 - 2S}{T}\left(\eta + \ln\frac{1-\eta}{1-\eta_0} - \eta_0\right)$$

and for $\mathbb{C}_2$ [15]:

$$t = \frac{\pi\eta_0^3\varkappa^2}{4n_0\mathfrak{T}}\int_{e_0}^{e}\frac{e}{\eta^3[\mathbf{E}(e)-\eta^2\mathbf{K}(e)]}$$
$$\times\left(\exp\int_{e_0}^{e}\frac{3x\mathbf{K}(x)dx}{2[\mathbf{E}(x)-(1-x^2)\mathbf{K}(x)]}\right)de,$$
$$a = a_0\left(\frac{\eta_0}{\eta}\right)^2\exp\left[\int_{e_0}^{e}\frac{e\mathbf{K}(e)de}{[\mathbf{E}(e)-\eta^2\mathbf{K}(e)]}\right],$$
$$i = i_0, \quad \Omega = \Omega_0, \tag{3}$$
$$\omega = \omega_0 + \int_{e_0}^{e}\left\{\frac{e\mathbf{K}(e)}{2[\mathbf{E}(e)-\eta^2\mathbf{K}(e)]}\frac{\mathfrak{R}}{\mathfrak{T}}\right\}de,$$
$$M = M_0 + \int_{e_0}^{e}\left\{\frac{\pi\varkappa^2 e}{4[\mathbf{E}(e)-\eta^2\mathbf{K}(e)]\mathfrak{T}}\right.$$
$$\left.+\frac{e\eta\mathbf{K}(e)}{2[\mathbf{E}(e)-\eta^2\mathbf{K}(e)]}\frac{\mathfrak{R}}{\mathfrak{T}}\right\}de.$$

Here and below, the subscript 0 marks the values of the variables at the initial epoch $t = 0$, e is the eccentricity, a is the semimajor axis, $n = \varkappa a^{-3/2}$ is the mean motion, $\eta = \sqrt{1-e^2}$, i is the imclination, Ω is the longitude of the ascending node, ω is the argument of the pericenter, and M is the mean anomaly. The standard notations for complete elliptic integrals in normal trigonometric form are also used [19]:

$$\mathbf{K}(e) = \int_0^{\pi/2}\frac{dx}{\sqrt{1-e^2\sin^2 x}},$$
$$\mathbf{E}(e) = \int_0^{\pi/2}\sqrt{1-e^2\sin^2 x}\,dx. \tag{4}$$

Solution (3) contains definite integrals from combinations of complete elliptic integrals, which can be found by numerical methods.

The first expression in systems (2) and (3) is a kinematic equation, which can be used to find the time during which a given change in eccentricity occurs, and, vice versa, by solving the kinematic equation $t(e) = \Delta t$ with respect to e, we can find the change in eccentricity over time Δt.

The definition domain of solutions of (2) and (3) is given in [14, 15]. The representations of these solutions are also provided there in the form of series expansions in powers of eccentricity. According to [16], in the case of solution (2), for reference frame $\mathcal{O}_1$ at $e \le 0.8$, it is necessary to use power-law series, so we present them here:

$$t = \frac{\varkappa^2}{n_0 T}\left[\sum_{k=0}^{\infty}\frac{(2k+1)!!}{(2k+2)!!}e_0^{2k}\right]^{-3}$$
$$\times\sum_{k=0}^{\infty}\left(\frac{(2k+3)!!}{(2k+4)!!}-\frac{1}{k+3}\right)\left(\frac{e^6}{e_0^6}e^{2k}-e_0^{2k}\right),$$
$$a = a_0\left(\frac{e}{e_0}\right)^4\left[\sum_{k=0}^{\infty}\frac{(2k+1)!!}{(2k+2)!!}e_0^{2k}\right]^{-2}$$
$$\times\left[\sum_{k=0}^{\infty}\frac{(2k+1)!!}{(2k+2)!!}e^{2k}\right]^2,$$
$$M = M_0 + \frac{\varkappa^2 - 2S}{T}$$
$$\times\left[2\ln\left(\frac{e}{e_0}\right)-\sum_{k=1}^{\infty}\frac{(2k-2)!}{2^{2k}(k!)^2}(e^{2k}-e_0^{2k})\right].$$

We also give a solution for a circular orbit, which is preferable to use instead of (2), (3) for $e \approx 0$:

$$a = a_0\left(1+\frac{t}{t_1}\right)^{2/3}, \quad i = i_0, \quad \Omega = \Omega_0, \quad \omega = \omega_0,$$
$$\lambda = \lambda_0 + n_0 t_1\left(1+\frac{2\mathfrak{R}}{\varkappa^2}\right)\ln\left(1+\frac{t}{t_1}\right) \quad \text{at} \quad t_1 = \frac{\varkappa^2}{3\mathfrak{T}n_0},$$

where $\lambda = \Omega + \omega + M$ is the mean longitude. This solution is also valid in reference frame $\mathbb{C}_1$ with replacement $\mathfrak{T} \to T$, $\mathfrak{R} \to -S$.

3. YARKOVSKY ACCELERATION MODEL

Within the linear thermophysical model of the Yarkovsky acceleration for spherical asteroids [17], the radial, transversal, and binormal components of this acceleration in the frame of reference $\mathbb{C}_1$ have the following form [18, Eq. (12)]:

$$P_r' = \frac{P_r}{r^2} = \frac{4\alpha\Phi}{9(1+\chi)}\{E_{R_s'}\sin(\delta_{R_s'}+\lambda)\sin\lambda\sin^2\gamma$$
$$+ E_{R_d'}\cos\delta_{R_d'}[\cos^2\lambda+\sin^2\lambda\cos^2\gamma]\},$$
$$P_t' = \frac{P_t}{r^2} = \frac{4\alpha\Phi}{9(1+\chi)}\{E_{R_s'}\sin(\delta_{R_s'}+\lambda)\cos\lambda\sin^2\gamma$$
$$- E_{R_d'}[\cos\delta_{R_d'}\sin\lambda\cos\lambda\sin^2\gamma+\sin\delta_{R_d'}\cos\gamma]\}, \tag{5}$$

$$P'_n = \frac{P_n}{r^2} = \frac{4\alpha\Phi}{9(1+\chi)}\{E_{R'_s}\sin(\delta_{R'_s}+\lambda)\sin\gamma\cos\gamma - E_{R'_d}[\cos\delta_{R'_d}\sin\lambda\sin\gamma\cos\gamma - \sin\delta_{R'_d}\cos\lambda\sin\gamma]\},$$

where the subscript s corresponds to the seasonal Yarkovsky effect, and d is the daily effect. In (5), γ is the obliquity of the asteroid's spin axis with respect to the normal to its orbital plane, $\lambda = \omega_{\rm rev}(t - t_0)$ is the mean longitude, $\omega_{\rm rev}$ is the mean motion, t is the time, t_0 is the initial time point, $\alpha = 1 - A$ is the optical absorption coefficient, A is the Bond albedo,

$$\Phi = \frac{\mathscr{E}_\star \pi R^2}{mc}, \quad \chi = \frac{\Theta_s}{\sqrt{2}R'_s}, \quad \Theta_s = \frac{\Gamma\sqrt{\omega_{\rm rev}}}{\epsilon\sigma T_\star^3},$$
$$\Gamma = \sqrt{K\rho C}, \quad T_\star = \left(\frac{\alpha\mathscr{E}_\star}{\epsilon\sigma}\right)^{1/4},$$

Γ is the thermal inertia of the surface, $T_\star$ is the temperature of the subsolar point, $\mathscr{E}_\star = L_\odot/(4\pi a^2)$ is the solar radiation flux at the heliocentric distance a, $L_\odot = 3.86\times10^{26}$ W is the luminosity of the Sun, $c = 299792458$ m/s is the speed of light, $\sigma = 5.670374419\times10^{-8}$ W m^{-2} K^{-4} is the Stefan–Boltzmann constant, m, R, ρ, ϵ, K, C are the mass, radius, bulk density, thermal emissivity, thermal conductivity, and specific heat capacity of the asteroid, respectively. Furthermore,

$$R'_s = \frac{R}{l_s}, \quad l_s = \frac{\Gamma}{\rho C\sqrt{\omega_{\rm rev}}}, \quad \omega_{\rm rev} = \frac{2\pi}{P_{\rm rev}},$$
$$R'_d = \frac{R}{l_d}, \quad l_d = l_s\sqrt{\frac{\omega_{\rm rev}}{\omega_{\rm rot}}}, \quad \omega_{\rm rot} = \frac{2\pi}{P_{\rm rot}},$$

where $P_{\rm rev}$ is the period of revolution of the asteroid around the Sun, and $P_{\rm rot}$ is the period of its rotation around the axis. In addition, the amplitude $E_{R'} = E(\sqrt{2}R')$ and phase $\delta_{R'} = \delta(\sqrt{2}R')$ are defined, like in [17], by the relations

$$E_{R'}\exp(i\delta_{R'}) = \frac{A(x) + iB(x)}{C(x) + iD(x)},$$
$$E_{R'}\exp(-i\delta_{R'}) = \frac{A(x) - iB(x)}{C(x) - iD(x)}, \quad (6)$$

where $i = \sqrt{-1}$, $x = \sqrt{2}R'$, and auxiliary functions

$$A(x) = -(x+2) - e^x[(x-2)\cos x - x\sin x],$$
$$B(x) = -x - e^x[x\cos x + (x-2)\sin x],$$
$$C(x) = A(x) + \frac{\chi}{1+\chi}\Big(3(x+2) + e^x[3(x-2)\cos x + x(x-3)\sin x]\Big),$$
$$D(x) = B(x) + \frac{\chi}{1+\chi}\Big(x(x+3) - e^x[x(x-3)\cos x - 3(x-2)\sin x]\Big).$$

Taking into account (6), we obtain

$$E_{R'}\cos\delta_{R'} = \frac{A(x)C(x) + B(x)D(x)}{C(x)^2 + D(x)^2},$$
$$E_{R'}\sin\delta_{R'} = \frac{B(x)C(x) - A(x)D(x)}{C(x)^2 + D(x)^2}. \quad (7)$$

The linear thermophysical model [17] was developed under simplifying assumptions of a circular orbit around the Sun and a spherical shape of the asteroid. For an elliptical orbit, the coefficient Φ will depend on the heliocentric distance r as $\Phi = (\Phi_0 r_0^2)/r^2$, where $r_0 = 1$ AU, and Φ_0 is Φ calculated for the distance of 1 AU. This inverse proportionality to the square of the distance is already included in our equations of motion (2) and (3) in accordance with the problem posed in the Introduction. Furthermore, we replace the mean longitude λ, which describes the position of the body in orbit, with the mean anomaly M and average the expressions for the tangential $P_{\mathfrak{T}}$ and normal $P_{\mathfrak{N}}$ components of vector $\mathbf{P}$ with respect to the mean anomaly over the orbital period. At the same time, we take into account that

$$P_{\mathfrak{T}} = P_r\sin f + P_t\cos f,$$
$$P_{\mathfrak{N}} = -P_r\cos f + P_t\sin f, \quad (8)$$

where P_r and P_t are the radial and transversal components of vector $\mathbf{P}$, f is the angle by which the velocity vector must be rotated to coincide with the transversal (Fig. 1),

$$\cos f = \frac{\eta}{\sqrt{1 - e^2\cos^2 E}}, \quad \sin f = \frac{e\sin E}{\sqrt{1 - e^2\cos^2 E}}, \quad (9)$$

E is the eccentric anomaly, and $M = E - e\sin E$.

While averaging, we assume that the orientation of the asteroid's axis of rotation and the periods $P_{\rm rev}$ and $P_{\rm rot}$ do not change with time.

Considering in (5) that $\Phi = (\Phi_0 r_0^2)/r^2$, we write the expressions for P_r and P_t in the form

$$P_r = \frac{2\alpha\Phi_0 r_0^2}{9(1+\chi)}\{E_{R'_s}\sin^2\gamma[\sin\delta_{R'_s}\sin 2M + \cos\delta_{R'_s}(1-\cos 2M)] + E_{R'_d}\cos\delta_{R'_d}[1 + \cos 2M + (1-\cos 2M)\cos^2\gamma]\}, \quad (10)$$

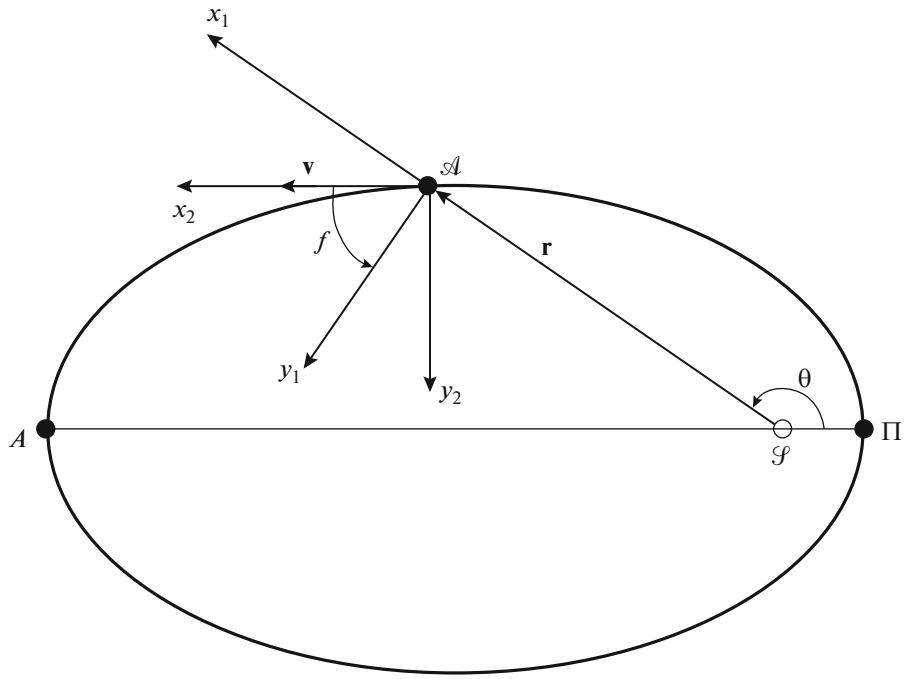

Fig. 1. The angle of rotation f of the velocity vector $\mathbf{v}$ until it coincides with the transversal. The axes of system $\mathbb{O}_1$ are radial x_1 and transversal y_1. The axes of system $\mathbb{O}_2$ are tangential x_2 and normal y_2. The binormal axes z_1 and z_2 are oriented toward us orthogonally to the orbital plane. The θ angle is the true anomaly.

$$P_t = \frac{2\alpha\Phi_0 r_0^2}{9(1+\chi)}\{E_{R_s'}\sin^2\gamma[\sin\delta_{R_s'}(1+\cos 2M) + \cos\delta_{R_s'}\sin 2M] - E_{R_d'}[\cos\delta_{R_d'}\sin 2M\sin^2\gamma + 2\sin\delta_{R_d'}\cos\gamma]\}.$$

Let us substitute (10) into (8) and combine similar terms:

$$P_{\mathfrak{T}} = \frac{2\alpha\Phi_0 r_0^2}{9(1+\chi)}\{E_{R_s'}\sin^2\gamma[\sin\delta_{R_s'}(\cos f + \cos 2M\cos f + \sin 2M\sin f) + \cos\delta_{R_s'}(\sin f - \cos 2M\sin f + \sin 2M\cos f)] + E_{R_d'}[\cos\delta_{R_d'}([1+\cos^2\gamma]\sin f + \sin^2\gamma[\cos 2M\sin f - \sin 2M\cos f]) - 2\sin\delta_{R_d'}\cos\gamma\cos f]\},$$

$$P_{\mathfrak{N}} = \frac{2\alpha\Phi_0 r_0^2}{9(1+\chi)}\{E_{R_s'}\sin^2\gamma[\sin\delta_{R_s'}(\cos 2M\sin f - \sin 2M\cos f + \sin f) + \cos\delta_{R_s'}(\sin 2M\sin f + \cos 2M\cos f - \cos f)] - E_{R_d'}[\cos\delta_{R_d'}([1+\cos^2\gamma]\cos f + \sin^2\gamma[\cos 2M\cos f + \sin 2M\sin f]) + 2\sin\delta_{R_d'}\cos\gamma\sin f]\}. \quad (12)$$

Let us carry out the averaging procedure of expressions (11) and (12):

$$\mathfrak{T} = \overline{P}_{\mathfrak{T}} = \frac{1}{2\pi}\int_0^{2\pi} P_{\mathfrak{T}}(M)dM = \frac{1}{2\pi}\int_0^{2\pi} P_{\mathfrak{T}}(E)(1-e\cos E)dE,$$

$$\mathfrak{N} = \overline{P}_{\mathfrak{N}} = \frac{1}{2\pi}\int_0^{2\pi} P_{\mathfrak{N}}(M)dM = \frac{1}{2\pi}\int_0^{2\pi} P_{\mathfrak{N}}(E)(1-e\cos E)dE,$$

and, considering the results given in Appendix A (Eqs. (A14)), we obtain the tangential and normal parameters:

$$\mathfrak{T} = \frac{2\alpha\Phi_0 r_0^2}{9\pi(1+\chi)}\left\{E_{R_s'}\sin\delta_{R_s'}\sin^2\gamma\left(2\eta\mathbf{K}(e) - \sum_{k=0}^{\infty} g_{1k}e^{2k}[2e^2(I_{k+1}-I_{k+2}) + \eta(2I_{k+1}-I_k)] + \sum_{k=0}^{\infty} g_{2k}e^{2k+2}(2I_{k+2}-I_{k+1}+2\eta(I_{k+2}-I_{k+1}))\right)\right. \quad (13)$$

$$- 4\eta \mathbf{K}(e) E_{R_d'} \sin\delta_{R_d'} \cos\gamma \Big\},$$

$$\Re = \frac{2\alpha\Phi_0 r_0^2}{9\pi(1+\chi)} \Big\{ E_{R_s'} \cos\delta_{R_s'} \sin^2\gamma \Big(-2\eta \mathbf{K}(e) + \sum_{k=0}^{\infty} g_{1k} e^{2k} [\eta(I_k - 2I_{k+1}) - 2e^2(I_{k+1} - I_{k+2})] - \sum_{k=0}^{\infty} g_{2k} e^{2k+2} [I_{k+1} - 2I_{k+2} + 2\eta(I_{k+1} - I_{k+2})] \Big) - E_{R_d'} \cos\delta_{R_d'} \Big[2\eta \mathbf{K}(e)(1+\cos^2\gamma) + \sin^2\gamma \sum_{k=0}^{\infty} g_{1k} e^{2k} [\eta(I_k - 2I_{k+1}) - 2e^2(I_{k+1} - I_{k+2})] - \sin^2\gamma \sum_{k=0}^{\infty} g_{2k} e^{2k+2} [2\eta(I_{k+1} - I_{k+2}) + I_{k+1} - 2I_{k+2}] \Big] \Big\}, \quad (14)$$

where $E_{R'} \cos\delta_{R'}$ and $E_{R'} \sin\delta_{R'}$ are defined by formulas (7), and I_k is expressed by the recursive formula:

$$I_k = \begin{cases} 2\mathbf{K}(e) & \text{at} \quad k = 0 \\ \dfrac{2}{e^2}[\mathbf{E}(e) - \eta^2 \mathbf{K}(e)] & \text{at} \quad k = 1 \\ \dfrac{(2e^2-1)(2k-2)}{e^2(2k-1)} I_{k-1} + \dfrac{(1-e^2)(2k-3)}{e^2(2k-1)} I_{k-2} & \text{at} \quad k > 1, \end{cases}$$

coefficients g_{1k} and g_{2k} are given in Appendix A (Eqs. (A7)), and their values for $k = 0$–15 are given in Table 4 in Appendix A.

The expressions for the radial, transversal, and binormal parameters were obtained in [16]. Let us write them in the following form:

$$S = \frac{2\alpha\Phi_0 r_0^2}{9(1+\chi)} \{ E_{R_s'} \cos\delta_{R_s'} \sin^2\gamma + E_{R_d'} \cos\delta_{R_d'} (1+\cos^2\gamma) \},$$
$$T = \frac{2\alpha\Phi_0 r_0^2}{9(1+\chi)} \{ E_{R_s'} \sin\delta_{R_s'} \sin^2\gamma - 2E_{R_d'} \sin\delta_{R_d'} \cos\gamma \}, \quad W = 0. \quad (15)$$

Comparing (13) and (14) with (15), we see that the tangential and normal parameters differ from the transversal and radial parameters in multiplying the daily and seasonal components by eccentricity-dependent coefficients. Taking into account the expression (A15) in the Appendix, we obtain $-\Re = S$, $\mathfrak{T} = T$ for $e = 0$, i.e., the trihedron (S, T, W) coincides with the trihedron $(-\Re, \mathfrak{T}, W)$ for circular orbits, as it should be. At $e = 1$, the elliptical orbit degenerates into rectilinear motion and the procedure of averaging over the orbital period loses its meaning; therefore, formulas (13)–(15) are inapplicable at $e = 1$.

Note 1. The radial S, transversal T, and binormal W parameters are analogues of non-gravitational parameters A_1, A_2, and A_3 [20]. They are related through the expressions $A_1 = S/r_0^2$, $A_2 = T/r_0^2$, $A_3 = W/r_0^2$, where $r_0 = 1$ AU.

Note 2. Expressions (13)–(15) allow us to estimate the magnitude of the Yarkovsky effect, but they require knowledge of such characteristics of the body as diameter, bulk density, rotation rate, obliquity of the spin axis to the orbital plane, Bond albedo, thermal inertia of the surface, specific heat capacity, and thermal emissivity.

4. EVOLUTION OF THE ORBITS OF MODEL ASTEROIDS

Let us consider model objects with different orbital eccentricities from 0 to 0.99, while all other orbital and thermophysical characteristics correspond to the asteroid 101955 Bennu (Table 1). We find the orbit-averaged values of the vector **P** components, the drifts of the elements, and the displacement relative to the unperturbed position in two frames of reference. The element drifts and displacement are marked with the subscript "1" if they are defined in reference frame $\mathbb{O}_1$, and "2" in reference frame $\mathbb{O}_2$.

For comparison, we will also calculate the drift of the mean anomaly and the displacement using the estimation formulas given in [21]:

$$\Delta M \simeq 0.01'' \dot{a}_4 (\Delta_{10} t)^2 a_{\mathrm{AU}}^{-5/2}, \quad (16)$$

$$\Delta\rho \simeq 7 \dot{a}_4 (\Delta_{10} t)^2 a_{\mathrm{AU}}^{-3/2} \text{ km}, \quad (17)$$

where ΔM is the variation in the mean anomaly in arcseconds; $\Delta\rho$ is the displacement in kilometers; $\dot{a}_4$ is the drift of the semimajor axis due to the Yarkovsky effect in units of 10^{-4} AU/Myr (the values are given in the eight column of Table 2); $\Delta_{10} t = 119.5479063961725$ is the time period for which the estimation is made in tens of years; and a_{AU} is the semimajor axis in astronomical units (Table 1). Estimates (16) and (17) were obtained in reference frame $\mathbb{O}_1$ neglecting the fourth-order terms in eccentricity.

Table 2 shows the tangential $\mathfrak{T}$ and normal $\Re$ parameters for different values of the initial eccentricity e_0. According to (15), the radial S and transversal T parameters do not depend on the eccentricity, $S = 9.91079 \times 10^{-14}$ AU^3/day^2, and $T = -5.10168 \times 10^{-14}$ AU^3/day^2 for all e_0. Figure 2 illustrates the difference of T from $\mathfrak{T}$ in percentage for $e_0 > 0.7$: at

Table 1. Orbital elements, thermophysical characteristics, and rotation parameters of asteroid 101955 Bennu

Parameter	Value	Ref.
Semi major axis a_0, AU	1.126391025894812	[20]
Mean motion n_0, deg/ day	0.8244613503320309	[20]
Inclination i_0, deg	6.03494377024794	[20]
Longitude of the ascending node Ω_0, deg	2.06086619569642	[20]
Argument of the pericenter ω_0, deg	66.22306084084298	[20]
Mean anomaly M_0, deg	101.703952002457	[20]
Period of revolution around the Sun $P_{\rm rev}$, days	436.6487281120201	[20]
Period of revolution around the Sun $P_{\rm rev}$, years	1.195479063961725	[20]
Thermal inertia Γ, J m^{-2} s$^{-1/2}$ K^{-1}	300	[12]
Specific heat C, J kg^{-1} K^{-1}	750	[9]
Thermal emissivity ϵ	0.95	[12]
Radius R, m	242.22	[12]
Period of rotation around the axis $P_{\rm rot}$, h	4.2960015	[12]
Bulk density ρ, kg m^{-3}	1194	[12]
Bond albedo A	0.0170	[22]
Right ascension of the pole α, deg	85.45218	[12]
Declination of the pole δ, deg	–60.36780	[12]
Obliquity of the spin axis γ, deg	177.53514	

Like in [12], we assume specific heat capacity $C = 750$ J kg^{-1} K^{-1} based on the measurements of CM-class meteorites (carbonaceous chondrites) [9]. γ is calculated from the equatorial coordinates of the pole in accordance with the method given in [23]. The epoch of the orbital elements is 2455562.5 (Jan. 1, 2011) TDB (JPL database accessed on February 3, 2022).

Table 2. Tangential $\mathfrak{T}$ and normal $\mathfrak{N}$ parameters, variations in the mean anomaly dM_1, dM_2 and semimajor axis da_1, da_2 for 1000 revolutions around the Sun (≈1195.48 years) depending on the initial eccentricity e_0

e_0	$\mathfrak{T}$, 10^{-14} AU^3/day^2	$\mathfrak{N}$, 10^{-14} AU^3/day^2	dM_1, arcmin	dM_2, arcmin	da_1, 10^{-4} AU	da_2, 10^{-4} AU	$\dot{a}_4$, 10^{-4} AU/Myr	ΔM, arcmin
0	–5.10168	–9.91079	35.083	35.083	–0.0244	–0.0244	–20.4226	36.126
0.001	–5.10168	–9.91079	35.083	35.091	–0.0244	–0.0244	–20.4226	36.126
0.01	–5.10155	–9.91054	35.086	35.094	–0.0244	–0.0244	–20.4246	36.130
0.05	–5.09849	–9.90457	35.169	35.179	–0.0245	–0.0245	–20.4738	36.217
0.10	–5.08887	–9.88585	35.436	35.445	–0.0246	–0.0246	–20.6289	36.491
0.20	–5.04976	–9.80969	36.541	36.544	–0.0254	–0.0254	–21.2735	37.631
0.30	–4.98212	–9.67805	38.555	38.511	–0.0268	–0.0268	–22.4424	39.699
0.40	–4.88179	–9.48280	41.767	41.592	–0.0291	–0.0289	–24.3125	43.007
0.50	–4.74156	–9.20998	46.783	46.252	–0.0325	–0.0322	–27.2298	48.168
0.60	–4.54897	–8.83547	54.827	53.404	–0.0381	–0.0371	–31.9094	56.445
0.70	–4.28099	–8.31451	68.808	65.068	–0.0478	–0.0452	–40.0414	70.830
0.80	–3.88832	–7.55138	97.475	86.772	–0.0678	–0.0603	–56.7181	100.330
0.85	–3.60997	–7.01056	126.470	106.582	–0.0879	–0.0741	–73.5681	130.137
0.90	–3.22864	–6.26976	184.719	142.155	–0.1284	–0.0988	–107.4058	189.993
0.95	–2.62669	–5.10050	359.973	230.430	–0.2503	–0.1602	–209.0021	369.709
0.97	–2.23295	–4.33575	593.878	326.187	–0.4129	–0.2268	–344.0411	608.583
0.99	–1.53792	–2.98595	1763.840	673.643	–1.2263	–0.4684	–1008.9714	1784.796

For all the e_0 values, the radial parameter $S = 9.91079 \times 10^{-14}$ AU^3/day^2, transversal parameter $T = -5.10168 \times 10^{-14}$ AU^3/day^2. Columns 8 and 9: $\dot{a}_4$ is the drift of the semimajor axis; ΔM is the variation in the mean anomaly calculated by formula (16) for 1000 orbital revolutions.

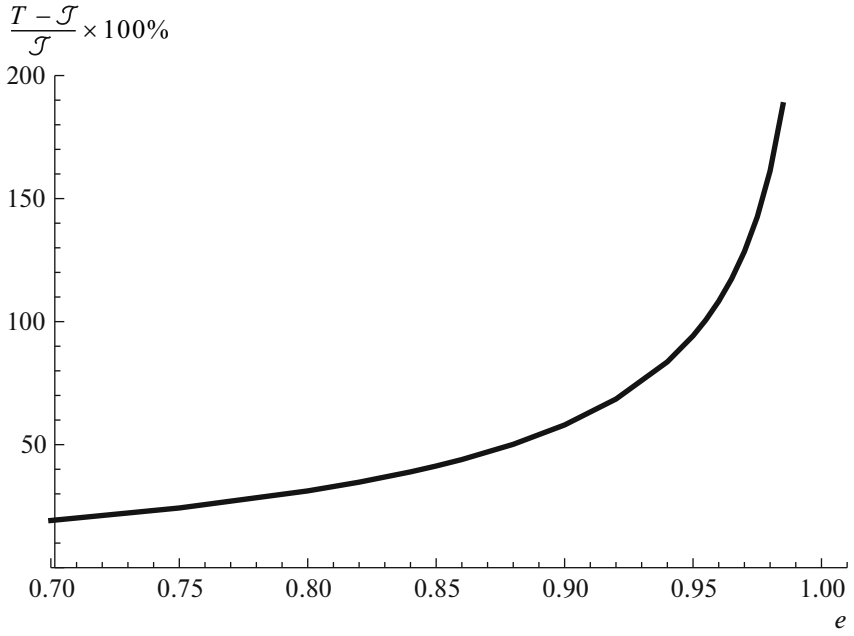

Fig. 2. The difference between the transversal parameter T and the tangential parameter $\mathfrak{T}$ in percentage at $e_0 > 0.7$.

$e_0 \in (0.7, 0.9)$ T exceeds $\mathfrak{T}$ by 19 to 58%, and in the interval $e_0 \in (0.9, 0.99)$ this difference is from 58 to 230%. The difference of S from $\mathfrak{R}$ behaves similarly.

Using the values of the acceleration components and formulas (2), (3), we find the variations in the mean anomaly dM_1, dM_2 and semimajor axis da_1, da_2 for 1000 revolutions around the Sun (≈1195.48 years) at different initial eccentricities e_0 (see Table 2). The differences of dM_1 from dM_2 and da_1 from da_2 are less than 1% for small eccentricities (up to 0.5). At e_0 from 0.5 to 0.7, their difference does not exceed 6%, gradually increasing with e_0. At $e_0 > 0.7$, these differences grow exponentially from 6 to 160%. The last column of Table 2 shows the variation in the mean anomaly calculated by formula (16). The comparison of columns dM_1 and ΔM gives good agreement between these values (the discrepancy does not exceed 3%).

Using the known formulas of celestial mechanics [24], we determine the displacement d of a small body relative to the unperturbed position, which will occur due to the Yarkovsky effect. For this purpose, we calculate the rectangular coordinates of the body from the unperturbed and perturbed orbital elements and then find the distance between these positions. Table 3 shows displacements d_1 and d_2 for 1000 orbital revolutions (≈1195.48 years) at various e_0, and Fig. 3 illustrates the difference of d_1 from d_2 in percentage at $e_0 > 0.7$. With an increase in the initial eccentricity from 0.7 to 0.9, the excess of displacement d_1 over d_2 changes from 6 to 30%, and at e_0 from 0.9 to 0.99, the difference is from 30 to 127%.

The calculation of displacement d_2 also considers the variation in the argument of pericenter $d\omega_2$; however, it is small (less than an arc second) over the considered period of time, and depends little on the eccentricity of the orbit. The variations in the eccentricity de_1, de_2 are small as well. If they are not considered, displacements d_1, d_2 will change by no more than 0.01%. Table 3 shows the differences $d_1 - d_1'$ and $d_2 - d_2'$, where d_1' and d_2' are the displacements calculated without taking into account de_1 and de_2. If the variation in the mean anomaly is also neglected, the displacement relative to the undisturbed position only due to a variation in the semimajor axis will be insignificant (columns d_1'' and d_2'' in Table 3). Also for comparison, the fifth column of Table 3 shows displacement $\Delta\rho$ calculated by formula (17). For $e_0 > 0.7$ the estimate $\Delta\rho$ exceeds d_1 by a factor of 1.65–3.2 and d_2 by a factor of 1.75–7.3, which indicates that the displacement estimate calculated by formula (17) can be significantly overestimated. This may explain the low detection of the Yarkovsky effect directly from astrometric observations: in the JPL database of small bodies, the parameter A_2 among NEAs less than 5 km in diameter was determined for 45 out of 588 objects with orbital eccentricities up to 0.5, and only for 18 out of 640 objects with $e > 0.5$, although the estimated value of the displacement at such eccentricities is greater, all other conditions being equal.

Table 3. Displacements d_1, d_2 of a small body relative to the unperturbed position for 1000 orbital revolutions (≈1195.48 years) depending on the initial eccentricity e_0

e_0	d_1, million km	$d_1 - d_1'$, km	d_1'', km	$\Delta\rho$, million km	d_2, million km	$d_2 - d_2'$, km	d_2'', km
0	1.71966	0.0	365.075	1.70907	1.71966	0.0	365.075
0.001	1.71928	0.178	365.149	1.70907	1.71930	0.357	365.149
0.01	1.71604	1.781	365.887	1.70924	1.71609	3.561	365.887
0.05	1.70196	8.824	370.565	1.71335	1.70209	17.632	370.564
0.10	1.68551	17.446	379.653	1.72633	1.68555	34.760	379.647
0.20	1.65829	34.101	409.154	1.78028	1.65802	67.165	409.049
0.30	1.64528	50.193	455.852	1.87809	1.64295	96.892	455.244
0.40	1.65490	66.235	524.900	2.03460	1.64752	124.061	522.577
0.50	1.70106	83.050	626.827	2.27873	1.68132	149.033	619.599
0.60	1.80741	101.888	783.857	2.67034	1.76016	172.153	763.404
0.70	2.02727	124.791	1048.942	3.35087	1.91706	193.350	991.838
0.80	2.51687	155.639	1582.061	4.74646	2.24191	210.957	1408.131
0.85	3.02407	176.492	2116.054	6.15655	2.55239	216.375	1783.212
0.90	4.04230	203.772	3184.583	8.98827	3.12305	215.809	2450.715
0.95	7.02744	242.184	6390.858	17.49037	4.56189	198.477	4090.901
0.97	10.80306	261.979	10666.079	28.79112	6.12077	177.893	5858.310
0.99	26.24914	269.915	32042.028	84.43589	11.55552	127.993	12238.077

Here, d_1' and d_2' are the displacements calculated without the drift of the eccentricity; d_1'' and d_2'' are the displacements calculated without the drifts of the eccentricity and the mean anomaly; $\Delta\rho$ is the displacement calculated by formula (17).

In system $\mathbb{O}_2$, parameters $\mathfrak{T}$ and $\mathfrak{N}$ gradually decrease with increasing e_0, but despite this decrease, the drifts of the elements and the displacement relative to the unperturbed position increase. In system $\mathbb{O}_1$, the growth of the element drifts and displacements with e_0 is much greater than in $\mathbb{O}_2$ for the same T and S for all e_0.

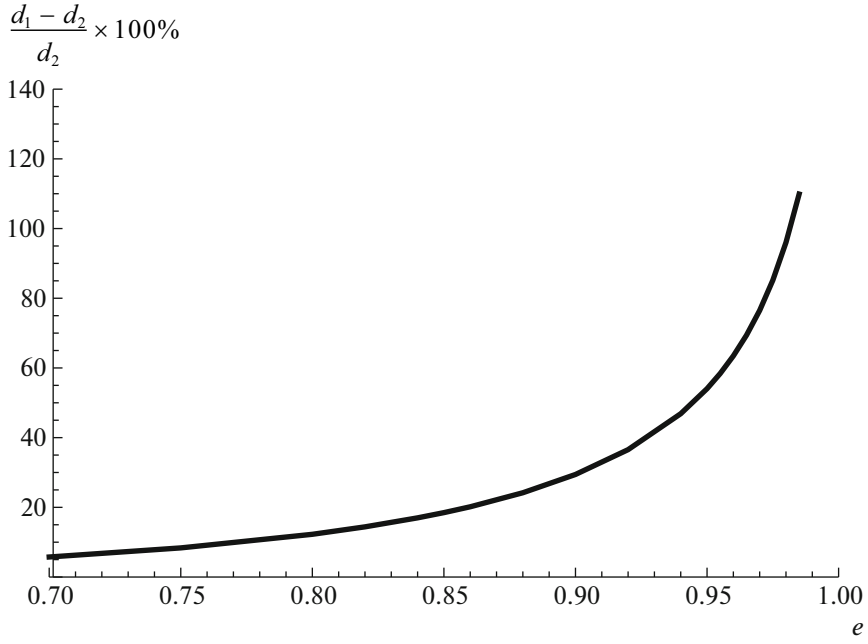

Fig. 3. The difference of displacement d_1 from displacement d_2 in percentage at $e_0 > 0.7$.

Thus, when the Yarkovsky effect is modeled by radial and transversal acceleration, the estimates of element drifts and displacement relative to the unperturbed position for objects with highly elliptical orbits may turn out to be overestimated. For such objects, it is necessary to develop special methods for taking into account the Yarkovsky effect.

5. CONCLUSIONS

Expressions for the mean values of the tangential and normal components of the Yarkovsky acceleration over the orbital period have been derived based on the rotation parameters and thermophysical characteristics of the asteroid in the linear thermophysical model of the Yarkovsky force for spherical asteroids. At $e \to 0$, $\mathfrak{T} \to T$, and $\mathfrak{N} \to -S$, as it should be. For an elliptical orbit, the tangential and normal parameters are always smaller in absolute value than the transversal and radial parameters, and their difference increases with orbital eccentricity. The drifts of the semimajor axis and the mean anomaly, as well as the displacements relative to the unperturbed position calculated for two orbital reference systems are almost identical at small eccentricities ($e_0 < 0.5$). When $e_0 > 0.5$, the values found in system $\mathbb{O}_1$ are always greater than the corresponding values in system $\mathbb{O}_2$. At e_0 from 0.5 to 0.7, the difference is moderate (<6%), but it gradually increases, and at $e > 0.7$, the differences in the drifts and displacement grow exponentially. Thus, when the Yarkovsky effect is modeled by radial and transversal acceleration, the estimates of element drifts and displacement relative to the unperturbed position for objects with highly elliptical orbits may be overestimated. For such objects, it is necessary to develop special methods for taking into account the Yarkovsky effect.

APPENDIX A

MEAN VALUES OF THE FUNCTIONS OF THE ECCENTRIC ANOMALY

The main part of the paper involves the mean values of the functions $\sin f$, $\cos f$, $\sin 2M \sin f$, $\sin 2M \cos f$, $\cos 2M \sin f$, and $\cos 2M \cos f$. All of them can be expressed explicitly as analytic 2π-periodic functions of the eccentric anomaly depending on the parameter e, $0 \le e < 1$. The functions $\sin f$, $\sin 2M \cos f$, and $\cos 2M \sin f$ are odd in E, because, according to (9),

$$\sin f = \frac{e \sin E}{\sqrt{1 - e^2 \cos^2 E}} = -\frac{e \sin(-E)}{\sqrt{1 - e^2 \cos^2(-E)}},$$
$$\sin 2M = \sin[2(E - e \sin E)]$$
$$= -\sin[2(-E - e \sin(-E))].$$

The mean value of the odd function is zero [24]. Therefore, we restrict ourselves to even functions for which the mean value is

$$\mathscr{E}w = \frac{1}{\pi}\int_0^\pi w dM = \frac{1}{\pi}\int_0^\pi w(1 - e\cos E)dE. \quad \text{(A1)}$$

The following properties may be useful:

$$\int_0^\pi w(\cos x)dx = 0, \quad \text{(A2)}$$
$$\text{if} \quad w(\cos x) = -w(-\cos x),$$

$$\int_0^\pi w(\cos x)dx = 2\int_0^{\pi/2} w(\cos x)dx, \quad \text{(A3)}$$
$$\text{if} \quad w(\cos x) = w(-\cos x).$$

Let us find the mean values of the functions we need. Taking into account (9), (A1), (A2), (A3), and (4),

$$\frac{1}{\pi}\int_0^\pi \cos f dM = \frac{1}{\pi}\int_0^\pi \frac{\eta}{\sqrt{1 - e^2\cos^2 E}}dE$$
$$-\frac{1}{\pi}\int_0^\pi \frac{e\eta\cos E}{\sqrt{1 - e^2\cos^2 E}}dE = \frac{2}{\pi}\int_0^{\pi/2} \frac{\eta}{\sqrt{1 - e^2\cos^2 E}}dE \quad \text{(A4)}$$
$$= \frac{2}{\pi}\int_{\pi/2}^\pi \frac{\eta}{\sqrt{1 - e^2\sin^2 x}}dx = \frac{2\eta}{\pi}\mathbf{K}(e),$$

where the new variable $x = E + \frac{\pi}{2}$. We express $\cos 2M$ and $\sin 2M$ through x and represent them as

$$\cos 2M = \cos[2(E - e\sin E)]$$
$$= -\cos(2x + 2e\cos x)$$
$$= -\cos 2x\sum_{k=0}^\infty g_{1k}e^{2k}\cos^{2k} x \quad \text{(A5)}$$
$$+ \sin 2x\sum_{k=0}^\infty g_{2k}e^{2k+1}\cos^{2k+1} x,$$

$$\sin 2M = \sin[2(E - e\sin E)]$$
$$= -\sin(2x + 2e\cos x)$$
$$= -\sin 2x\sum_{k=0}^\infty g_{1k}e^{2k}\cos^{2k} x \quad \text{(A6)}$$
$$- \cos 2x\sum_{k=0}^\infty g_{2k}e^{2k+1}\cos^{2k+1} x,$$

where

$$g_{1k} = (-1)^k\frac{2^{2k}}{(2k)!}, \quad g_{2k} = (-1)^k\frac{2^{2k+1}}{(2k+1)!}. \quad \text{(A7)}$$

Expansions (A5) and (A6) were obtained using standard formulas for adding angles and expanding trigonometric functions in power-law series [19]. The values of the coefficients g_{1k}, g_{2k} for $k = 0$–15 are given in

Table 4. Values g_{1k}, g_{2k} as rational (top) and decimal (bottom) fractions

k	g_{1k}	g_{2k}	k	g_{1k}	g_{2k}
0	1	2	8	$\frac{2}{638\,512\,875}$	$\frac{4}{10\,854\,718\,875}$
	1.0	2.0		3.13×10^{-9}	3.69×10^{-10}
1	-2	$-\frac{4}{3}$	9	$-\frac{4}{97\,692\,469\,875}$	$-\frac{8}{1\,856\,156\,927\,625}$
	-2.0	-1.3333		-4.09×10^{-11}	-4.31×10^{-12}
2	$\frac{2}{3}$	$\frac{4}{15}$	10	$\frac{4}{9\,280\,784\,638\,125}$	$\frac{8}{194\,896\,477\,400\,625}$
	0.6667	0.2667		4.31×10^{-13}	4.10×10^{-14}
3	$-\frac{4}{45}$	$-\frac{8}{315}$	11	$-\frac{8}{2143861251406875}$	$-\frac{16}{49\,308\,808\,782\,358\,125}$
	-0.0889	-0.0254		-3.73×10^{-15}	-3.24×10^{-16}
4	$\frac{2}{315}$	$\frac{4}{2835}$	12	$\frac{4}{147\,926\,426\,347\,074\,375}$	$\frac{8}{3\,698\,160\,658\,676\,859\,375}$
	0.0063	0.0014		2.70×10^{-17}	2.16×10^{-18}
5	$-\frac{4}{14175}$	$-\frac{8}{155925}$	13	$-\frac{8}{48\,076\,088\,562\,799\,171\,875}$	$-\frac{16}{1\,298\,054\,391\,195\,577\,640\,625}$
	-2.82×10^{-4}	-5.13×10^{-5}		-1.66×10^{-19}	-1.23×10^{-20}
6	$\frac{4}{467\,775}$	$\frac{8}{6\,081\,075}$	14	$\frac{8}{9\,086\,380\,738\,369\,043\,484\,375}$	$\frac{16}{263\,505\,041\,412\,702\,261\,046\,875}$
	8.55×10^{-6}	1.32×10^{-6}		8.80×10^{-22}	6.07×10^{-23}
7	$-\frac{8}{42\,567\,525}$	$-\frac{16}{638\,512\,875}$	15	$-\frac{16}{3\,952\,575\,621\,190\,533\,915\,703\,125}$	$-\frac{32}{122\,529\,844\,256\,906\,551\,386\,796\,875}$
	-1.88×10^{-7}	-2.51×10^{-8}		-4.05×10^{-24}	-2.61×10^{-25}

Table 4 in the form of rational and decimal fractions, which will allow us to judge their behavior. The sum symbols in (A5) and (A6) have an infinite upper limit, but since the coefficients rapidly decrease with the growth of k, in practice it is sufficient to use 15–20 terms. Expansions into a series of functions $\cos(2e\cos x)$ and $\sin(2e\cos x)$ converge for any values of $2e\cos x$: $-\infty < 2e\cos x < \infty$, hence they converge for all $e \in [0,1]$.

Taking into account (9), (A1), and (A5), as well as the commutativity of the integration and summation operations, we find

$$\frac{1}{\pi}\int_0^{\pi}\cos 2M\cos f dM$$
$$= -\frac{\eta}{\pi}\sum_{k=0}^{\infty} g_{1k}e^{2k}\int_{\pi/2}^{3\pi/2}\frac{\cos 2x\cos^{2k}x}{\sqrt{1-e^2\sin^2 x}}dx$$
$$+\frac{\eta}{\pi}\sum_{k=0}^{\infty} g_{2k}e^{2k+1}\int_{\pi/2}^{3\pi/2}\frac{\sin 2x\cos^{2k+1}x}{\sqrt{1-e^2\sin^2 x}}dx \qquad \text{(A8)}$$
$$+\frac{\eta}{\pi}\sum_{k=0}^{\infty} g_{1k}e^{2k+1}\int_{\pi/2}^{3\pi/2}\frac{\sin x\cos 2x\cos^{2k}x}{\sqrt{1-e^2\sin^2 x}}dx$$
$$-\frac{\eta}{\pi}\sum_{k=0}^{\infty} g_{2k}e^{2k+2}\int_{\pi/2}^{3\pi/2}\frac{\sin x\sin 2x\cos^{2k+1}x}{\sqrt{1-e^2\sin^2 x}}dx.$$

By passing back to E, it is easy to show that, by virtue of (A2), the second and third terms in expression (A8) are zero. After small trigonometric transformations, we bring (A8) to the form

$$\frac{1}{\pi}\int_0^{\pi}\cos 2M\cos f dM$$
$$= \frac{\eta}{\pi}\sum_{k=0}^{\infty} g_{1k}e^{2k}\int_{\pi/2}^{3\pi/2}\frac{\cos^{2k}x - 2\cos^{2k+2}x}{\sqrt{1-e^2\sin^2 x}}dx \qquad \text{(A9)}$$
$$-\frac{2\eta}{\pi}\sum_{k=0}^{\infty} g_{2k}e^{2k+2}\int_{\pi/2}^{3\pi/2}\frac{\cos^{2k+2}x - \cos^{2k+4}x}{\sqrt{1-e^2\sin^2 x}}dx.$$

Similarly, we obtain

$$\frac{1}{\pi}\int_0^{\pi}\sin 2M\sin fdM$$
$$=\frac{1}{\pi}\sum_{k=0}^{\infty}g_{1k}e^{2k+1}\int_{\pi/2}^{3\pi/2}\frac{\sin 2x\cos^{2k+1}x}{\sqrt{1-e^2\sin^2 x}}dx$$
$$-\frac{1}{\pi}\sum_{k=0}^{\infty}g_{1k}e^{2k+2}\int_{\pi/2}^{3\pi/2}\frac{\sin x\sin 2x\cos^{2k+1}x}{\sqrt{1-e^2\sin^2 x}}dx$$
$$+\frac{1}{\pi}\sum_{k=0}^{\infty}g_{2k}e^{2k+2}\int_{\pi/2}^{3\pi/2}\frac{\cos 2x\cos^{2k+2}x}{\sqrt{1-e^2\sin^2 x}}dx$$
$$-\frac{1}{\pi}\sum_{k=1}^{\infty}g_{2k}e^{2k+3}\int_{\pi/2}^{3\pi/2}\frac{\sin x\cos 2x\cos^{2k+2}x}{\sqrt{1-e^2\sin^2 x}}dx,$$

where the first and last terms are zero. As a result,

$$\frac{1}{\pi}\int_0^{\pi}\sin 2M\sin fdM$$
$$=-\frac{2}{\pi}\sum_{k=0}^{\infty}g_{1k}e^{2k+2}\int_{\pi/2}^{3\pi/2}\frac{(\cos^{2k+2}x-\cos^{2k+4}x)}{\sqrt{1-e^2\sin^2 x}}dx \quad \text{(A10)}$$
$$-\frac{1}{\pi}\sum_{k=0}^{\infty}g_{2k}e^{2k+2}\int_{\pi/2}^{3\pi/2}\frac{(\cos^{2k+2}x-2\cos^{2k+4}x)}{\sqrt{1-e^2\sin^2 x}}dx.$$

Thus, finding the necessary mean values is reduced to the integrals of the form

$$I_k=\int_{\pi/2}^{3\pi/2}\frac{\cos^{2k}x}{\sqrt{1-e^2\sin^2 x}}dx \quad \text{at} \quad k\geq 0. \quad \text{(A11)}$$

In [19], the following formula is given:

$$\int\frac{\cos^n x}{\sqrt{1-k^2\sin^2 x}}dx=\frac{\cos^{n-3}x}{(n-1)k^2}\sin x\sqrt{1-k^2\sin^2 x}$$
$$+\frac{n-2}{n-1}\frac{2k^2-1}{k^2}\int\frac{\cos^{n-2}x}{\sqrt{1-k^2\sin^2 x}}dx$$
$$+\frac{n-3}{n-1}\frac{1-k^2}{k^2}\int\frac{\cos^{n-4}x}{\sqrt{1-k^2\sin^2 x}}dx,$$

with the help of which we obtain the recursive relation for calculating (A11):

$$I_k=\frac{2k-2}{2k-1}\frac{2e^2-1}{e^2}I_{k-1}+\frac{2k-3}{2k-1}\frac{1-e^2}{e^2}I_{k-2}. \quad \text{(A12)}$$

The first terms of the I_k sequence are easy to find using the reference book [19]:

$$I_0=\int_{\pi/2}^{3\pi/2}\frac{dx}{\sqrt{1-e^2\sin^2 x}}=2\mathbf{K}(e),$$
$$I_1=\int_{\pi/2}^{3\pi/2}\frac{\cos^2 xdx}{\sqrt{1-e^2\sin^2 x}}=\frac{2}{e^2}[\mathbf{E}(e)-\eta^2\mathbf{K}(e)]. \quad \text{(A13)}$$

Taking into account (A4), (A9), (A10), and (A11), we write the final expressions for the desired mean values:

$$\frac{1}{\pi}\int_0^{\pi}\cos fdM=\frac{2\eta}{\pi}\mathbf{K}(e),$$
$$\frac{1}{\pi}\int_0^{\pi}\cos 2M\cos fdM=\frac{\eta}{\pi}\sum_{k=0}^{\infty}g_{1k}e^{2k}(I_k-2I_{k+1})$$
$$-\frac{2\eta}{\pi}\sum_{k=0}^{\infty}g_{2k}e^{2k+2}(I_{k+1}-I_{k+2}), \quad \text{(A14)}$$
$$\frac{1}{\pi}\int_0^{\pi}\sin 2M\sin fdM=-\frac{2}{\pi}\sum_{k=0}^{\infty}g_{1k}e^{2k+2}(I_{k+1}-I_{k+2})$$
$$-\frac{1}{\pi}\sum_{k=0}^{\infty}g_{2k}e^{2k+2}(I_{k+1}-2I_{k+2}).$$

Let us consider the behavior of the integrals (A14) for $e=0$. The last two expressions on the right contain the uncertainty of the form $0:0$ due to (A12) and (A13). Therefore, we set $e=0$ in the original integrals and calculate them:

$$\frac{1}{\pi}\int_0^{\pi}\cos fdM=\frac{1}{\pi}\int_0^{\pi}dE=1,$$
$$\frac{1}{\pi}\int_0^{\pi}\cos 2M\cos fdM=\frac{1}{\pi}\int_0^{\pi}\cos 2EdE=0, \quad \text{(A15)}$$
$$\frac{1}{\pi}\int_0^{\pi}\sin 2M\sin fdM=0.$$

FUNDING

The study was carried out as part of the state assignment "Investigation of Objects of Near-Earth Space."

CONFLICT OF INTEREST

The author declares that she has no conflicts of interest.

REFERENCES

1. D. Farnocchia, S. R. Chesley, D. Vokrouhlický, A. Milani, F. Spoto, and W. F. Bottke, Icarus **224**, 1 (2013).

2. C. Tardioli, D. Farnocchia, B. Rozitis, D. Cotto-Figueroa, S. R. Chesley, T. S. Statler, and M. Vasile, Astron. Astrophys. **608**, A61 (2017).
3. A. del Vigna, L. Faggioli, A. Milani, F. Spoto, D. Farnocchia, and B. Carry, Astron. Astrophys. **617**, A61 (2018).
4. T. Yu. Galushina and O. M. Syusina, Russ. Phys. J. **63**, 420 (2020).
5. V. A. Shor, O. M. Kochetova, L. L. Sokolov, and Yu. A. Chernetenko, in *Asteroid-Comet Hazard: Yesterday, Today, Tomorrow,* Ed. by B. M. Shustov and L. V. Rykhlova (Fizmatlit, Moscow, 2010), Chap. 7 [in Russian].
6. J. Ďurech, M. Delbó, B. Carry, J. Hanuš, and V. Ali-Lagoa, Astron. Astrophys. **604**, A27 (2017).
7. J. Ďurech, D. Vokrouhlický, P. Pravec, J. Hanuš, et al., Astron. Astrophys. **609**, A86 (2018).
8. J. R. Masiero, C. Nugent, A. K. Mainzer, E. L. Wright, et al., Astron. J. **154**, 168 (2017).
9. C. P. Opeil, D. T. Britt, R. J. Macke, and G. J. Consolmagno, Meteor. Planet. Sci. **55** (8), E1 (2020).
10. S. Tachibana, H. Sawada, R. Okazaki, Y. Takano, et al., Science (Washington, DC, U. S.) **375** (6584), 1011 (2022).
11. D. S. Lauretta, A. E. Bartels, M. A. Barucci, E. B. Bierhaus, et al., Meteor. Planet Sci. **50**, 834 (2015).
12. M. G. Daly, O. S. Barnouin, J. A. Seabrook, J. Roberts, et al., Sci. Adv. **6** (41), eabd3649 (2020).
13. T. N. Sannikova and K. V. Kholshevnikov, Astron. Rep. **63**, 420 (2019).
14. T. N. Sannikova and K. V. Kholshevnikov, Astron. Rep. **64**, 778 (2020).
15. T. N. Sannikova, Astron. Rep. **65**, 1265 (2021).
16. T. N. Sannikova, Astron. Rep. **65**, 312 (2021).
17. D. Vokrouhlický, Astron. Astrophys. **344**, 362 (1999).
18. Y.-B. Xu, L-Y. Zhou, C. Lhotka, and W.-H. Ip, Mon. Not. R. Astron. Soc. **493**, 1447 (2020).
19. I. S. Gradshtein and I. M. Ryzhik, *Tables of Integrals, Series, and Products* (BKhV-Peterburg, St. Petersburg, 2011; Elsevier Inc., Burlington, 2007).
20. JPL Small-Body Database Search Engine, Jet Propulsion Laboratory NASA. https://ssd.jpl.nasa.gov/sbdb_query.cgi
21. D. Vokrouhlický, A. Milani, and S. R. Chesley, Icarus **148**, 118 (2000).
22. C. W. Hergenrother, C. K. Maleszewski, M. C. Nolan, J.-Y. Li, et al., Nat. Commun. **10**, 1291 (2019).
23. C. Lhotka, J. Souchay, and A. Shahsavari, Astron. Astrophys. **556**, A8 (2013).
24. K. V. Kholshevnikov and V. B. Titov, *Two Body Problem* (SPbGU, St. Petersburg, 2007) [in Russian].

Translated by M. Chubarova